IL NUOVO CIMENTO **42 C** (2019) 223
DOI 10.1393/ncc/i2019-19223-6

COMMUNICATIONS: SIF Congress 2018

Testing gravity with atomic quantum sensors

L. SALVI

Dipartimento di Fisica e Astronomia and LENS, Università di Firenze, INFN Sezione di Firenze Via Sansone 1, 50019 Sesto Fiorentino, Italy

received 15 February 2019

Summary. — In this article, three experiments aimed at the detection of gravitational effects with atomic sensors are reported. In the first experiment, a gradiometer is used to perform a precision measurement of the Newtonian gravitational constant G. In the second experiment, a similar apparatus is used to provide a test of the Weak Equivalence Principle for atoms in different internal states and in a coherent superposition of internal states. Finally, in the third experiment, a new kind of interferometer operating on a single-photon transition is described. This sensor is a promising candidate for the detection of low-frequency gravitational waves.

1. – Introduction

Atoms can be used as sensors to probe gravitational interactions owing to their non-zero mass. When the temperature of an atomic ensemble is reduced to values close to absolute zero, the quantum wave nature of matter emerges, which makes it possible to perform interference experiments that are sensitive to gravity [1]. Similarly to light optics, the main ingredient for the operation of atomic interferometers is coherence, that is, the existence of a well defined phase of the matter wave.

While matter objects are used in light interferometry to split and reflect laser beams, in atom interferometry it is possible to use laser beams to split and reflect matter waves. Splitting and reflection of matter waves can be performed in a number of ways that exploit the interaction of light with atoms. One option is to shine laser light onto atoms with a frequency matching that of an atomic resonance. It is well-known that this leads to Rabi oscillations in the population of the states involved in the transition. If the interaction parameters —namely the radiation intensity and the time duration— are properly tuned, one can produce a coherent superposition of two states (a beam splitter) or a population inversion (a mirror). A laser interaction that produces an equal superposition of two states is named a $\pi/2$ pulse whereas an interaction that produces population inversion is known as a π pulse because of the conditions imposed on the product $\Omega\tau$ between the Rabi frequency and the interaction time. For atoms travelling in free space, the

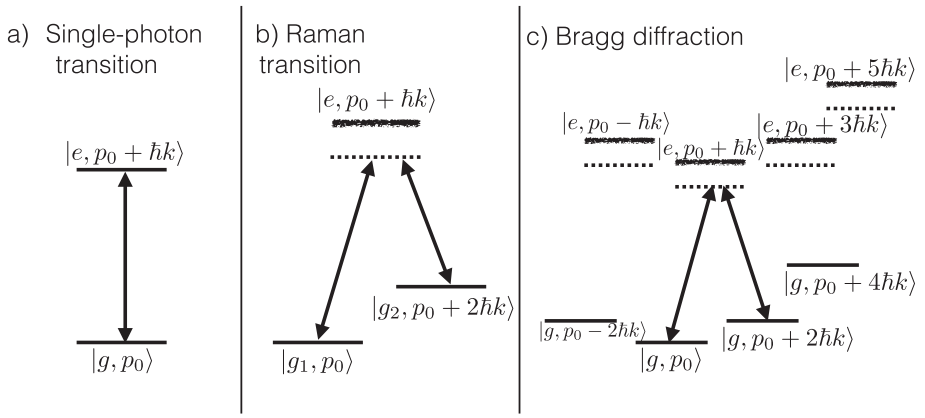

Fig. 1. – Three options that allow to implement the beam splitters and mirrors in an atom interferometer. The double arrows indicate the incident lasers' frequencies. The horizontal lines represent stable atomic states while the fuzzy lines represent states with a short lifetime. (a) A single-photon transition that requires a single laser frequency and two long-lived states. (b) A two-photon Raman transition between the states $|g_1, p_0\rangle$ and $|g_2, p_0 + 2\hbar k\rangle$ via the excited state $|e, p_0 + \hbar k\rangle$. (c) A first-order Bragg transition between states that only differ by the center-of-mass momentum.

absorption or the emission of a photon occurring in a Rabi oscillation lead to the recoil of the atom making it possible to split and reflect matter waves in real space.

While a single-photon transition as the one now described appears as the simplest choice for an atom interferometer, it seldom represents a practical option because optically excited states often have a limited lifetime of a few nanoseconds, a situation that would severly limit the duration of the interferometer. An interesting exception to this statement will be discussed in sect. **4**. In most cases, however, multiphoton transitions are used that only involve stable substates of the atomic ground level. This is the case, for example, in stimulated Raman transitions for which the initial and final states differ by the internal excitation and by the external (center-of-mass) motion [2, 3]. A similar situation occurs for Bragg diffraction, the matter-wave analog of the diffraction of X-rays off a crystal. In this case, multi-photon transitions can be driven that involve states only differing by the external motion [4, 5]. A schematic representation of these three options that can be used to implement the interferometer transitions is shown in fig. 1.

One of the most common interferometer arrangements is the Mach-Zehnder interferometer, a scheme where a matter wave is split, reflected and recombined. An illustration of such a device is shown in fig. 2. While in the optical interferometer, the accumulated phase difference between the two arms is detected as a count rate difference between two photodetectors at the output, in the atomic version it is estimated through the measured population difference between the two states exiting the interferometer. As stated at the beginning of this introduction, the main difference between these two setups lies in the pronounced sensitivity of the atomic interferometer to gravitational interactions. In the simplest example of a uniform gravity field with acceleration g, it can be shown that the accumulated phase shift is given by the expression [6]

$$\Phi = k_{\text{eff}} g T^2 + (\phi_1 - 2\phi_2 + \phi_3), \tag{1}$$

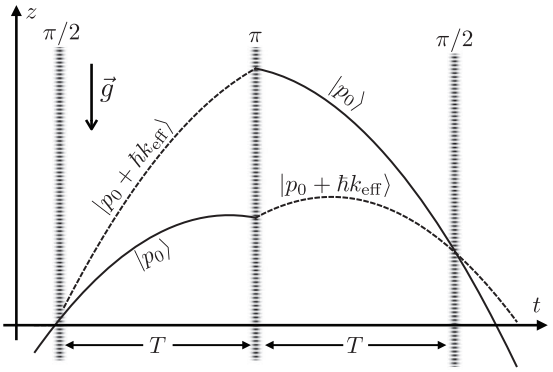

Fig. 2. – Scheme of the Mach-Zehnder atom interferometer in the presence of gravity acceleration g. Because of the beam splitter ($\pi/2$) and mirror (π) pulses, the atomic trajectories separate spatially. Absorption of one or more photons causes the transition between momentum states $|p_0\rangle \rightarrow |p_0 + \hbar k_{\rm eff}\rangle$ whereas stimulated emission causes the transition $|p_0 + \hbar k_{\rm eff}\rangle \rightarrow |p_0\rangle$. At the output of the interferometer, at $t > 2T$, the accumulated phase shift is estimated by measuring the population difference between the two states.

where T is the time interval between interferometer pulses, $\hbar k_{\rm eff}$ is the effective momentum transferred by the pulses to the atoms and ϕ_1, ϕ_2, ϕ_3 are the laser phases at the first, second and third pulses, respectively. The quantity $\hbar k_{\rm eff}$ corresponds to the momentum of a single photon in the case of a direct optical transition or to the sum of the photon momenta exchanged in a multi-photon transition. Despite its simplicity, eq. (1) sums up quite well most of the effort that is necessary to increase the sensitivity to accelerations. Indeed, maximizing the *signal* Φ requires exchanging multiple photon momenta and requires increasing the interferometer duration $2T$. On the other hand, the phase shift is estimated through a population measurement, a process that contains intrinsic noise due to the projection of quantum superpositions onto the basis of the interferometer states [7]. When the particles are uncorrelated, this noise sets a lower boundary to the attainable phase resolution $\Delta\Phi = 1/\sqrt{N}$, known as the atom shot noise, where N is the number of atoms. As a result, the effort of improving the phase resolution translates into increasing the atom flux and into the generation of multi-particle entanglement that can improve the atom number scaling of the phase resolution [8].

The atom shot noise limit can be reached in current state-of-the-art interferometers [9] and an example of this situation will be discussed in the following. However, depending on the specific setup, one must face significant challenges to reach this level. Indeed, the simple accelerometer really acts as a ruler —made up of the laser wavefronts—that imprints the laser phase onto the atoms, as shown by the presence of the phases ϕ_i in eq. (1). As a result, any laser fluctuation or wavefront imperfection will add noise to the interferometer. Many noise sources like these can be largely suppressed in gradiometer configurations where the phase shift difference between two interferomters sharing the same (imperfect) laser is measured. Electromagnetic interactions can also cause uncertainties because, despite the atoms being neutral, they possess charge distributions that are subject to forces. In this sense, it is meaningful to choose the atomic species and the transitions in order to avoid this sensitivity [10, 11].

In this article, three experiments are described that take advantage of the cancellation in the gradiometer configuration of many sources of uncertainty and that can sense

gravitational interactions. The first is a gradiometer that can sense the presence of nearby source masses thereby providing a measurement of the Newtonian gravitational constant. The second is a gradiometer operated in order to measure the difference in the free fall rate of two atomic clouds in different internal states so as to yield a test of the quantum version of the equivalence principle. In a third experiment, a single-photon transition connecting two long-lived states is used to implement a gravimeter and a gradiometer that is potentially insensitive to laser phase noise for arbitrarily large cloud separations. Because of this feature, this new kind of interferometer is a promising candidate for the detection of low-frequency gravitational waves.

2. – Measurement of the Newtonian gravitational constant

Despite the numerous past measurements [12] and importance of the Newtonian gravitational constant G, this remains the least known fundamental constant. The reasons for this poor knowledge of G lie in the intrinsic weakness of the gravitational interaction and in the impossibility of screening it so that any mass in the surroundings of an apparatus can potentially contribute to the measurement. On the other hand, theory cannot provide a link between gravity and the other forces nor it can give a prediction of its strength. As a consequence of these difficulties, since the first experiment by Cavendish in 1798 [13], the precision in the measurement of G improved by only two orders of magnitude in over two centuries and there exist large discrepancies between measurement results. A common feature of all experiments performed so far is the use of macroscopic masses both for the field source and for the field sensor. The aim of the MAGIA experiment developed and performed in Florence between 2002 and 2013 was to provide an independent measurement of G using cold atoms instead of macroscopic masses as field sensors [9, 14, 15]. The advantages of this approach lie in the high reproducibility and high control of atomic properties as well as in the achievable high sensitivity to gravity of atom interferometers.

The idea of the experiment is the implementation of an atom interferometer based on two-photon Raman transitions operated in the gradiometer configuration. The instrument is arranged in order to sense the gravity gradient generated by nearby tungsten cylinders whose height is modulated so as to extract the interferometer phase shift due to those masses only. The main part of the setup is shown in fig. 3(a).

The atomic source is formed by ^{87}Rb atoms trapped in a magneto-optical trap (MOT) at a temperature of $4\,\mu$K. The atoms are vertically launched in the interferometer tube (surrounded by the tungsten masses) with the same MOT laser beams, using the moving molasses technique. The Raman system is formed by two lasers entering the interferometer region from below and retroreflected by a mirror above the vacuum system, thus forming two couples of counterpropagating beams. These lasers are tuned to the two-photon resonance of the $F = 1 \leftrightarrow F = 2$ transition of the rubidium hyperfine structure. Using this method, a narrow atomic velocity class is selected with a width of 2.6 mm/s [16], corresponding to a temperature of 70 nK, and an atom number of 10^5–10^6. The same Raman beams are then used to perform the Mach-Zehnder $\pi/2$-π-$\pi/2$ pulse sequence on the two clouds of the gradiometer. With a total interferometer time $2T = 320$ ms, a signal-to-noise ratio of 10^3 in the detection of the interference fringe was obtained. Remarkably, this number corresponds to atom shot noise-limited sensitivity for 10^6 atoms and leads to a sensitivity to gravity of $10^{-9}\,g$, after averaging for one second. In the presence of the tungsten source masses, formed by 24 cylinders with a total mass

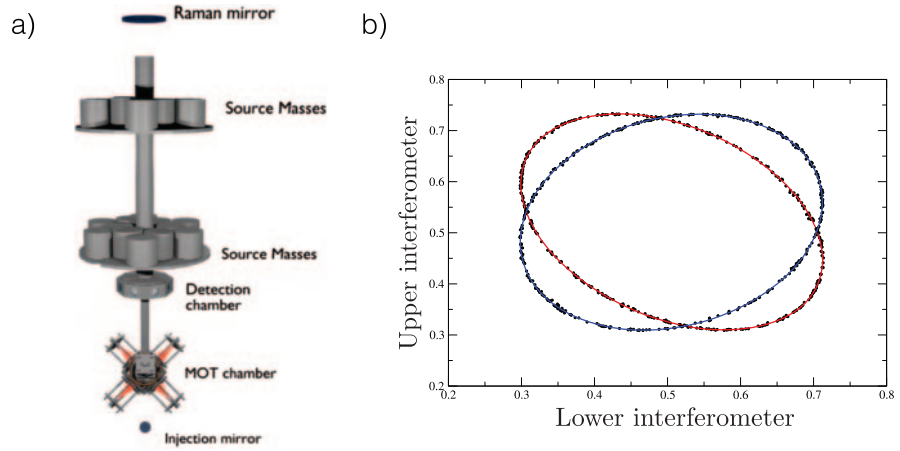

Fig. 3. – (a) Setup of the MAGIA experiment with the MOT chamber and the interferometer tube surrounded by the tungsten source masses. (b) Relative populations of the two interferometers in the gradiometer. The points lie on two ellipses corresponding to two positions of the masses relative to the atoms.

of 516 kg, the added acceleration is $5 \times 10^{-8}\, g$. In these conditions, averaging for 100 hours led the instrument to a relative precision of 10^{-4} for the measurement of G.

There is however a number of systematic effects that should be taken into account before the correct value of G is extracted. One very important effect arises from the Coriolis force which, because of the Earth's rotation and because of the atomic transverse velocity distribution, can cause shifts and loss of fringe contrast. However, since the reference frame for the gravity measurement is given by the upper Raman mirror, a rotation applied to the mirror can compensate the Coriolis shift. A very important source of uncertainty is the atomic trajectory. Indeed, because the field of the masses is position-dependent, it is essential to precisely characterize the atomic positions during the interferometer. Among all systematic effects, this uncertainty is the main limit to the determination of G. Many other systematic effects such as light shifts and wavefront distortions could be suppressed by reversing the sign of the momentum transfer to the atoms. This cancellation works because many shifts are either even or odd in the momentum transfer. In the MAGIA experiment, the reversal could be achieved simply by tuning the Raman beams' frequencies thus selecting a particular couple of beams that resonates with the atoms.

The effort spent in realizing this experiment led to the suppression of systematic shifts to the level of 92 ppm (parts per million) whereas the shot noise contribution is 116 ppm. Aside from improving the determination of the main systematic shifts in this measurement, this remarkable result shows that it is meaningful to either increase the atom flux or attempt to beat the shot noise limit with entangled states.

3. – Quantum test of the Weak Equivalence Principle

The same apparatus described for the measurement of the Newtonian constant can also provide a test of the Weak Equivalence Principle (WEP), also known as the universality of free fall. The Principle states that the trajectory of a chargeless body is independent of its internal structure and composition. Equivalently, for a given object,

the Principle states the numerical equality between its weight, given by the gravitational mass m_g and its inertia, given by the inertial mass m_i. Violations of the WEP are quantified in terms of the Eötvös parameter η, given by the difference of the accelerations $a_A - a_B$ of two objects with different internal structure and composition, normalized to the average acceleration:

$$\eta = \left| \frac{a_A - a_B}{(a_A + a_B)/2} \right| = 2 \left| \frac{(m_i/m_g)_A - (m_i/m_g)_B}{(m_i/m_g)_A + (m_i/m_g)_B} \right|. \tag{2}$$

Many experiments with macroscopic masses have been performed to date that provide stringent tests of the universality of free fall. These experiments involved torsion balances [17] and lunar laser ranging measurements [18]. Finally, the record is currently set by the MICROSCOPE space mission [19] whose preliminary data constrain the Eötvös parameter to less than about 10^{-14}. There naturally is a substantial interest in testing the WEP with quantum objects such as atoms instead of microscopic masses. Indeed, in this case, not only one can employ different species but tests can also be performed with particles in different states of their internal excitation. As a result, there is a generation of experiments aiming at testing the WEP with atoms thus providing limiting values of η in the range 10^{-7}–10^{-8} [20-24]. All these measurements can however be interpreted in terms of classical tests. One of the distinctive features of quantum mechanics is the existence of coherent superpositions of atomic states and one might ask whether particles in these states fall at the same rate as a particle in an eigenstate of the internal Hamiltonian. While in the classical case we say that if the WEP is valid, then the ratio m_g/m_i must be unity, in the quantum case we must consider inertial and gravitational mass operators $\hat{M}_i$ and $\hat{M}_g$ and say that the product $\hat{M}_g \hat{M}_i^{-1}$ must equal the identity. Possible deviations from this behavior will be represented, for a system with two internal states, as

$$\hat{M}_g \hat{M}_i^{-1} = \begin{pmatrix} r_1 & r \\ r^* & r_2 \end{pmatrix}. \tag{3}$$

In this expression $r_1 = r_2 = 1$ and $r = 0$ if the quantum WEP is valid. Different values of r_1 and r_2 indicate violations of the classical WEP whereas non-zero values of r indicate violations of the quantum version of the WEP.

In the experiment performed in our group [25], the two atomic states considered are the hyperfine levels $|F = 1, m_F = 0\rangle \equiv |1\rangle$ and $|F = 2, m_F = 0\rangle \equiv |2\rangle$ of the ^{87}Rb atom. Similarly to the determination of the Newtonian constant, the difference of accelerations between atoms in different states is determined with a two-cloud interferometer in the gradiometer configuration. In particular, the beam splitters and mirrors are realized through third-order Bragg diffraction so that each single cloud remains in the same internal state for the duration of the interferometer. Three accelerations enter the measurement: for a cloud in state $|i\rangle$, the acceleration is gr_i, for $i = 1, 2$. On the other hand, for a cloud in the equal superposition state $|s\rangle = (|1\rangle + e^{i\phi_s}|2\rangle)/\sqrt{2}$, the measured acceleration is

$$a_s = g \left[\frac{r_1 + r_2}{2} + |r| \cos(\phi_s + \phi_r) \right], \tag{4}$$

where $r = |r|e^{i\phi_r}$. In the experiment, a microwave at the frequency of the $|1\rangle \leftrightarrow |2\rangle$ hyperfine transition induces the superposition $|s\rangle$ with a phase ϕ_s that varies randomly

from one experiment cycle to the other. In the experiment, a reference phase shift Φ_{11} is measured by operating the interferometer with the two clouds in the same state $|1\rangle$. The classical version of the WEP is then tested by measuring Φ_{12}, the interferometer phase when the two clouds are in the different states $|1\rangle$ and $|2\rangle$, which is proportional to $r_1 - r_2$. Finally, the quantum version of the WEP is tested by measuring Φ_{1s}, *i.e.,* the differential acceleration of a cloud in state $|1\rangle$ and a cloud in state $|s\rangle$. In this case, the presence of a non-zero value of r is observable as an excess phase noise because of the dependence on the noisy phase ϕ_s in eq. (4).

The results of these measurements could limit violations of the classical WEP to the level $\eta = (1.4 \pm 2.8) \times 10^{-9}$, a result almost two orders of magnitude better than previous ones obtained for atoms in different electronic states. For the comparison of the accelerations between atoms in state $|1\rangle$ and atoms in state $|s\rangle$, the limit to quantum WEP violations was found to be $\eta_s = (3.3 \pm 2.9) \times 10^{-9}$. Finally, the measurements could provide limits on the value of $|r|$. Indeed, by attributing all the observed noise in Φ_{1s} to quantum WEP violations, it is possible to see that $|r| < 5 \times 10^{-8}$.

4. – Atom Interferometry on a single-photon transition

In the two experiments previously described, multi-photon transitions are used to implement the beam splitters and mirrors of the Mach-Zehnder interferometer. This choice avoids many problems related to the finite lifetime of optically excited states and the only effect of these states lies in off-resonance scattering. An interferometer operated on a single-photon transition, on the other hand, requires the existence of a long-lived excited state because, during the interferometer, the atoms must spend time in the excited state. In this situation, two difficulties emerge: first, if the lifetime of the excited state is long, the optical transition must have a narrow linewidth and second, a narrow linewidth implies a weak interaction with laser fields. Technically, these difficulties imply that an ultra-stable and high-power laser is necessary.

Despite these challenges, an interferometer operating on such an optical clock transition has a considerable advantage over Raman and Bragg interferometers [26, 27]. To understand this point let us first consider a gradiometer operating on a two-photon transition induced by counterpropagating waves, where each of the two clouds is close to the laser sources. When the separation L between the sensors is large, the pulses from the two sides must be sent with a time delay L/c so that they temporally overlap at the positions of the clouds and induce the transition. Because of this delay, the laser's phase noise will add to the differential interferometer phase and cause a background for gravity signals at frequencies higher than c/L, which amounts to 30 kHz when $L = 10$ km. This noise is instead absent when the gradiometer is operated on a single-photon transition. In this case, the photon phase is set at the time of emission from the source and accumulates no further noise in the path from one cloud to the other, provided that this path is in vacuum.

These considerations gain relevance in the design of gravitational wave (GW) detectors where extremely large baselines are required to attain the necessary strain sensitivity. Such a detector would sense the passage of a GW through the variation of the length L that would shift the phase impressed onto the atoms. The interest of atom interferometers as GW detectors lies in the capability of covering a frequency range (1 mHz–10 Hz) where optical interferometers have a smaller sensitivity.

In our group, a proof-of-principle implementation of a gradiometer operating on a single-photon transition was realized [28]. In this experiment, the $^1S_0$-$^3P_0$ optical clock

transition of ^{88}Sr at 698 nm was used to implement the beam splitters and mirrors. The laser light was generated by a semiconductor laser system consisting of an extended-cavity diode laser (ECDL), a slave laser as a preamplifier and a tapered amplifier. The light of the ECDL was stabilized by locking to a high-finesse ultra-stable cavity. With these stabilization and amplification stages, it is possible to send about 80 mW of optical power to the atoms, with a laser linewidth of about 1 Hz.

In the first experiments performed with this new kind of sensor, a gravimeter was implemented. In this configuration, strontium atoms were laser cooled in a MOT, trapped and released from an optical lattice and velocity selected by a π pulse of the clock laser, finally achieving about 10^4 atoms at an effective temperature of about 1 nK. After velocity selection, the Mach-Zehnder interferometer sequence was performed with interaction times up to $2T = 10$ ms. The results showed that, as expected, the interferometer is sensitive to the laser's phase noise. This includes the intrinsic laser phase fluctuations as well as all the vibrations of the optical components in the path to the atoms. While many of these noise sources are extremely hard to remove or reduce, the noise cancellation technique applied to a 10 m fiber bringing the light to the atoms showed an improvement of the fringe visibility, as can be seen from the data in fig. 4.

The most interesting application of the interferometer operated on the optical clock transition is the gradiometer because of the reasons stated at the beginning of this section. This configuration should indeed lead to results that are opposite to the gravimeter in terms of sensitivity to laser phase noise. Here, a double lattice launch was implemented, where a fraction of the atoms from the MOT is first trapped and launched through an optical lattice and a part of the residual free-falling atoms is subsequently trapped and launched in a second stage of the optical lattice. At the end of this procedure, two atomic clouds with about 10^5 atoms each are launched with a separation of 1.9 mm and a velocity difference of 3.4 cm/s. Again, after velocity selection, about 10^4 atoms per cloud are selected and the Mach-Zehnder gradiometer sequence is performed. Because of the small interaction times T that were possible in our setup, the phase shift difference between the two accelerometers due to gravity gradients alone was too small to be detected. Characterizing the sensitivity of the interferometer was however possible because of the velocity difference between the two clouds and the pronounced velocity selectiv-

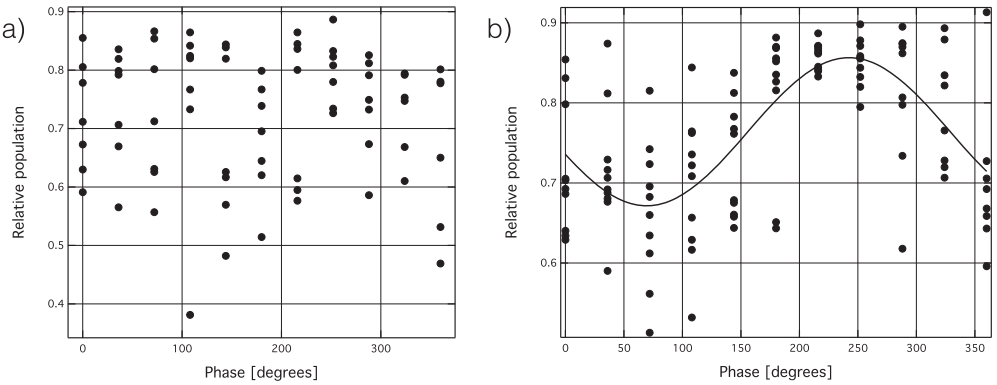

Fig. 4. – Interference fringes of the gravimeter operated on the clock transition for an interaction time $2T = 10$ ms. (a) In the presence of the fiber noise, the fringe cannot be distinguished. (b) With the fiber noise cancellation setup the fringe becomes visible as the fit (solid line) shows.

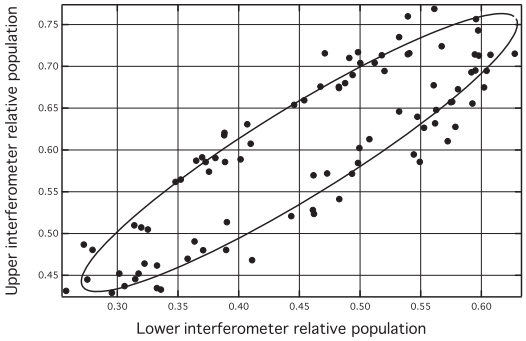

Fig. 5. – Ellipse recorded in the gradiometer configuration by plotting the interference fringe of the upper interferometer *vs.* the fringe of the lower interferometer, in the presence of the added artificial phase shift.

ity of the clock transition. As a result, we drove an acousto-optic modulator with two radiofrequency (RF) components so that the two corresponding optical frequencies could interact with the two clouds. Aside from providing the possibility of interacting with the two clouds simultaneously despite the velocity difference, this method also allows to imprint an artificial phase shift onto the gradiometer simply by tuning the relative phase of the two RF components. With this added tuning capability, it was possible to establish that the gradiometer for $2T = 10\,\mathrm{ms}$ is largely insensitive to laser phase noise and that, with our apparatus, the sensitivity was only a factor five worse than the atom shot noise limit. The data for the interference fringes of the upper interferometer *vs.* the lower one are shown in fig. 5. From this plot, the correlation of the fringes in the differential configuration is evident.

5. – Conclusions

In this article, three experiments that can sense gravitational effects were described. In the first two experiments, a rubidium gradiometer was used both to provide the first precision measurement of the Newtonian constant G and to provide the first test of the quantum version of the WEP. In the third experiment, performed with strontium atoms, an interferometer operating on a single-photon transition was implemented, showing effective laser noise cancellation in the gradiometer configuration and showing that this type of sensor is indeed a good candidate for the detection of low-frequency gravitational waves. In these three experiments, the atom shot noise limit of phase estimation was either reached or approached. As a result, it is meaningful to study and implement schemes that can produce metrologically useful entangled states. In this group, considerable effort is now devoted to the implementation of a Bragg diffraction-based spin squeezed interferometer with strontium atoms [29], also motivated by recent progress in the production of squeezed states of alkaline-earth-like atoms [30]. Additionally, the strontium optical clock transition is being considered for tests of the WEP with optically separated states.

* * *

The author acknowledges the members of the group of Guglielmo M. Tino who have contributed to the work described in this article. This work was supported by INFN and

the Italian Ministry of Education, University and Research (MIUR) under the Progetto Premiale Interferometro Atomico and the PRIN 2015 project Interferometro Atomico Avanzato per Esperimenti su Gravità e Fisica Quantistica e Applicazioni alla Geofisica.

REFERENCES

[1] Tino G. M. and Kasevich M. A. (Editors), *Atom Interferometry* (Società Italiana di Fisica and IOS Press, Amsterdam) 2014.
[2] Kasevich M. and Chu S., *Phys. Rev. Lett.*, **67** (1991) 181.
[3] Peters A., Chung K. Y. and Chu S., *Nature*, **400** (1999) 849.
[4] Müller H., Chiow S.-w., Long Q., Herrmann S. and Chu S., *Phys. Rev. Lett.*, **100** (2008) 180405.
[5] Kovachy T., Asenbaum P., Overstreet C., Donnelly C. A., Dickerson S. M., Sugarbaker A., Hogan J. M., and Kasevich M. A., *Nature*, **528** (2015) 530
[6] Storey P. and Cohen-Tannoudji C., *J. Phys. II (France)*, **4** (1994) 1999.
[7] Itano W. M., Bergquist J. C., Bollinger J. J., Gilligan J. M., Heinzen D. J., Moore F. L., Raizen M. G. and D. J. Wineland, *Phys. Rev. A*, **47** (1993) 3554.
[8] Giovannetti V., Lloyd S. and Maccone L., *Phys. Rev. Lett.*, **96** (2006) 010401.
[9] Sorrentino F., Bodart Q., Cacciapuoti L., Lien Y.-H., Prevedelli M., Rosi G., Salvi L. and Tino G. M., *Phys. Rev. A*, **89** (2014) 023607.
[10] Mazzoni T., Zhang X., Del Aguila R., Salvi L., Poli N. and Tino G. M., *Phys. Rev. A*, **92** (2015) 053619.
[11] del Aguila R. P., Mazzoni T., Hu L., Salvi L., Tino G. M. and Poli N., *New J. Phys.*, **20** (2018) 043002.
[12] Quinn T., *Nature*, **408** (2000) 919.
[13] Cavendish H., *Philos. Trans. R. Soc. London*, **88** (1798) 469.
[14] Rosi G., Sorrentino F., Cacciapuoti L., Prevedelli M. and Tino G. M., *Nature*, **510** (2014) 518.
[15] Prevedelli M., Cacciapuoti L., Rosi G., Sorrentino F. and Tino G. M., *Philos. Trans. R. Soc. A*, **372** (2014) 20140030.
[16] Moler K., Weiss D. S., Kasevich M. and Chu S., *Phys. Rev. A*, **45** (1992) 342.
[17] Wagner T. A., Schlamminger S., Gundlach J. H. and Adelberger E. G., *Class. Quantum Grav.*, **29** (2012) 184002.
[18] Williams J. G., Turyshev S. G. and Boggs D. H., *Class. Quantum Grav.*, **29** (2012) 184004.
[19] Touboul P. *et al.*, *Phys. Rev. Lett.*, **119** (2017) 231101.
[20] Fray S., Diez C. A., Hänsch T. W. and Weitz M., *Phys. Rev. Lett.*, **93** (2004) 240404.
[21] Bonnin A., Zahzam N., Bidel Y. and Bresson A., *Phys. Rev. A*, **88** (2013) 043615.
[22] Zhou L. *et al.*, *Phys. Rev. Lett.*, **115** (2015) 013004.
[23] Schlippert D., *Phys. Rev. Lett.*, **112** (2014) 203002.
[24] Tarallo M. G. *et al.*, *Phys. Rev. Lett.*, **113** (2014) 023005.
[25] Rosi G., D'Amico G., Cacciapuoti L., Sorrentino F., Prevedelli M., Zych M., Brukner Č. and Tino G., *Nat. Commun.*, **8** (2017) 15529.
[26] Dimopoulos S., Graham P. W., Hogan J. M., Kasevich M. A. and Rajendran S., *Phys. Lett. B*, **678** (2009) 37.
[27] Graham P. W., Hogan J. M., Kasevich M. A. and Rajendran S., *Phys. Rev. Lett.*, **110** (2013) 171102.
[28] Hu L., Poli N., Salvi L. and Tino G. M., *Phys. Rev. Lett.*, **119** (2017) 263601.
[29] Salvi L., Poli N., Vuletić V. and Tino G. M., *Phys. Rev. Lett.*, **120** (2018) 033601.
[30] Braverman B. *et al.*, *Phys. Rev. Lett.*, **122** (2019) 223203.